J. Nannoplankton Res., **38**(1), 2020, pp. 57–79
ISSN 1210-8049 Printed by The Sheridan Press, USA

Middle Eocene to Early Oligocene calcareous nannofossils from the Nanggulan Formation, Java, Indonesia

Amy P. Jones, Tom Dunkley Jones
School of Geography, Earth and Environmental Science, University of Birmingham, Edgbaston, Birmingham B15 2TT, UK; APJ527@student.bham.ac.uk, t.dunkleyjones@bham.ac.uk

Manuscript received 15th May, 2019; revised manuscript accepted 28th June, 2020

Abstract In this article, we document the late Middle Eocene to Early Oligocene calcareous nannofossil assemblages from a new low-latitude site in the south-central region of Java, Indonesia. The studied assemblages are from the Nanggulan Formation, recovered from cores drilled in the Special Region of Yogyakarta. The study focused on a ~60-m succession of marine clays and claystones that were recovered from Corehole NKK1, which includes a near-continuous Eocene–Oligocene section. The Late Eocene palaeolocation of this site was close to the region of the modelled peak sea-surface temperatures of the Eocene Indo-Pacific Warm Pool. Documenting coccolithophore communities from the tropical ocean through an interval of global cooling is important for several reasons. In particular, the Late Eocene to Early Oligocene coccolithophore assemblages of NKK1 include species that are usually only found in younger Oligocene assemblages, suggesting that this region may have been a key location for coccolithophore speciation and a source of increased diversity. Conversely, there were no significant range extensions of Lower or Middle Eocene taxa up-section, suggesting a degree of synchrony in extinctions across the tropical to subtropical oceans. A total of 115 species are documented, and two new species—*Coccolithus aspida* and *Reticulofenestra nanggulanensis*—are described.

Keywords Eocene, Oligocene, Java, taxonomy, calcareous nannofossils, biostratigraphy

1. Introduction

Calcareous nannofossils were examined from sediment cores that were recovered in 2006 from the Middle Eocene to Lower Oligocene portion of the Nanggulan Formation of Java. The cores were taken from drill-site NKK1, near the village of Nanggulan, in the Special Region of Yogyakarta (-7.788555˚S, 110.20578˚E; Figure 1). A full description of the drilling operations, sedimentology and integrated biostratigraphy is ongoing (Coxall et al., unpublished data, 2019). Sediments from these cores contain abundant and well-preserved calcareous nannofossils. The sedimentary sequences in NKK1 span the upper Middle Eocene to Lower Oligocene, including a continuous record of the Eocene–Oligocene Transition (EOT), and can be used to generate new records of tropical nannoplankton ecology and biostratigraphy through this critical interval of Earth history. Today, Java is located within the Indo-Pacific Warm Pool (IPWP), which extends from the western waters of the equatorial Pacific Ocean, through the Indo-Australian Archipelago (IAA) and into the eastern Indian Ocean. The extent of the IPWP is defined by ocean surface-waters with year-round temperatures exceeding 28˚C. In the modern climate system, these are the warmest surface ocean-waters in the world (De Deckker, 2016). In the Eocene, climate models have suggested that the IPWP was both warmer *and* covered a larger region of the Indo-Pacific Ocean than today (Huber & Caballero, 2011; Lunt et al., 2012). Palaeogeographic reconstructions (Hall, 2009, 2012, 2013) have placed NKK1 at the centre of this palaeo-IPWP during the Late Eocene. Today, the IAA is the tropical centre of maximum diversity in marine benthic communities (Renema et al., 2008).

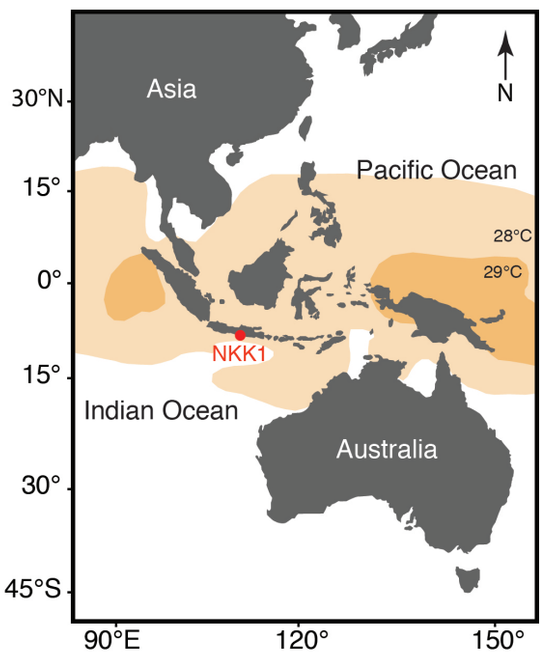

Figure 1: Present day map of Eastern Asia, Indonesia and Australia, depicting the modern IPWP temperature gradients (orange) and the location of core NKK1 in the southern region of Java

Fossil and molecular evidence indicate that these diversity hotspots have moved over the past ~50 Myr, in conjunction with major tectonic events (Renema et al., 2008). During the Eocene, neither Java nor the IAA were areas of maximum invertebrate biodiversity (Renema et al., 2008). However, the Eocene equatorial Indian Ocean region, including the East African margin, has recorded higher species diversities than other, contemporary fossil communities at similar tropical latitudes (Renema et al., 2008). For the plankton, and especially the calcareous phytoplankton, exceptionally-preserved Middle Eocene fossil assemblages from the tropical East African margin record peak species diversities (Bown et al., 2008). It is not clear whether these high diversities are a product of exceptional preservation or reflect a primary biogeographic diversity hotspot for calcareous phytoplankton in the tropical Indo-Pacific Ocean. The taxonomic assessment of calcareous nannofossil assemblages from Java, close to the centre of the palaeo-IPWP, help to address these questions of latitudinal and spatial diversity gradients of microplankton in the Middle and Late Eocene.

During the Late Eocene to Early Oligocene, and especially across the EOT, there was a long-term decline in the diversity of calcareous phytoplankton species (Bown et al., 2004). High-resolution studies of this transition have shown a gradual, progressive loss of species in the central (Fioroni et al., 2015) and eastern (Dunkley Jones et al., 2008) Indian Ocean. The current study, from the central IPWP, has enabled the development of detailed assemblage and biostratigraphic records that test the nature of species loss and extinction diachroneity across the tropical Indo-Pacific. Here, we test the recently-proposed biostratigraphic zonation schemes developed for the mid-latitudes (Agnini et al., 2014) in a tropical low-latitude region close to conditions of peak ocean warmth. The zonation of Agnini et al. (2014) included events based on the evolution and extinction of species in the *Reticulofenestra reticulata* group, in which there are subtle taxonomic discriminations across a group of morphologically-similar or intergrading species. We sought to test these species concepts in Late Eocene 'tropical endmember' assemblages as a way of assessing the recently-proposed bioevents, given the known extinction diachroneity in this group (Berggren et al., 1995; Villa et al., 2008; Persico et al., 2012).

2. Geological setting

During the Middle Eocene, Australia and Antarctica began to separate as Australia migrated northwards. This placed the Java region in a convergent tectonic regime that reinitiated Cretaceous subduction zones around the Sunda Arc, an active margin on the southerly side of Sundaland (Hall, 2009, 2012). Extensive islands and shallow seas were created (Hall, 2012, 2013) by subduction of the Australian and Pacific Plates below the continental part of Southeast Asia (Hall, 2012). Southeast Asia increased in size through the addition of continental fragments that rifted away from Australia and were subsequently added to the margins of Sundaland (Hall, 2009). Palaeogeographic reconstructions of Sundaland (the Malay Peninsula, Sumatra, Java, Borneo and surrounding small islands) during the Palaeogene are subject to some uncertainty (Hall, 2013), but they indicate an Eocene palaeolatitude for NKK1 of ~-6.5°S, which is not dissimilar to the position of Java today (Hall, 2012; Figure 1).

NKK1 was positioned to maximise the recovery of the Middle Eocene to Oligocene sediments of the Nanggulan Formation that crops out northwest of the village of Kenteng, on the eastern flank of the Menoreh Hills. NKK1 penetrated a total depth of 100 m, and core recovery was >90% for most of the Watu Puru Beds and the Jetis Beds of the Nanggulan Formation. Barren horizons or poorly-preserved nannofossil assemblages occurred in sediments both immediately below and for an interval of ~3 m above a basalt unit at ~40 m in the core. Nannofossil preservation and recovery was more variable in the Lower to Middle Oligocene upper Jetis Beds and Tegalsari Marls that occur above the basalt horizon, and none of this material was included in the current study. We focused on core samples between 41.04 and 99.98 m below ground level (mbgl), including samples NKK1-30 to NKK1-82, interpreted as belonging to calcareous nannofossil Zones CNE15–CNO3 of Agnini et al. (2014), equivalent to Zones NP17–NP23 of Martini (1971).

3. Sampling and methods

Sixty-five sediment samples were collected from NKK1 for calcareous nannofossil analysis. They were prepared using the simple smear-slide technique of Bown & Young (1998). Specimens were observed using a Zeiss AxioScope in cross-polarised light (XPL) at x1250 magnification. Images were captured using QImaging and QCap-

ture Pro 7 software. Calcareous nannofossil preservation and abundances were determined for all samples using a standard semiquantitative scale, where abundance was A – abundant (>10–100 specimens per field of view [FOV]), C – common (>1–10 specimens per FOV), F – few (1 specimen per 1–10 FOV), and preservation was G – excellent/good (little/no dissolution and/or recrystallisation, primary morphological characteristics slightly altered, specimens identifiable to species level), M – moderate (minimal etching and/or recrystallisation, primary morphological characteristics somewhat altered, most specimens identifiable to species level), P – poor (badly etched/overgrown, primary morphological characteristics mostly destroyed, with fragmentation and specimens not identifiable to species/genus level).

Nannofossil assemblage composition data for NKK1 from the Middle Eocene to Lower Oligocene can be found on figshare (https://doi.org/10.6084/m9.figshare.12488783.v1) in the form of a range-chart for all samples studied. At least 400 specimens were counted from each sample, followed by an additional scan of at least two transects of each slide, in order to maximise the identification of rare species. Any species noted outside of the count are represented by an asterisk (*) in the chart.

4. Biostratigraphy

The biostratigraphic interpretation of the NKK1 samples (Figure 2) employed the calibrated bioevents of Agnini et al. (2014); both the Agnini et al. (2014) and Martini (1971) biozonation schemes are shown for reference in Table 1. All ages were adjusted to the Geologic Timescale 2012 (Gradstein et al., 2012). Establishing robust bioevents for biozonation schemes for the Late Eocene has been difficult. Of those bioevents proposed by Martini (1971), the bases of *Sphenolithus pseudoradians* and *Isthmolithus recurvus* are diachronous across latitudes, and *I. recurvus* is entirely absent from tropical environments (Wei & Wise, 1990; Dunkley Jones et al., 2008, 2009; Fioroni et al., 2015). Agnini et al. (2014) sought to remedy this lack of reliable bioevents with the addition of a series of events based on the *R.* (*Cribrocentrum*) *reticulata* lineage. The successive appearances and extinctions of these typically tropical to subtropical species through the Late Eocene has the potential to significantly improve low- to mid-latitude nannofossil biozonations. However, one possible complicating factor involves the morphotypes in the *R. reticulata* lineage. Fornaciari et al. (2010) defined two new species—*Cribrocentrum* (*Reticulofenestra*) *isabellae* for large (>12 μm) forms with narrow central-areas and *C. erbae* with a broad tube and distinctly closed central-area. Agnini et al. (2014) used both species as biohorizon marker taxa, but it is not clear how their revised taxonomy relates to previous biostratigraphic studies that did not make any distinction between the morphotypes of *R. reticulata*. Here, we carefully examined the variability in the *R. reticulata* lineage, with the purpose of refining the existing taxonomy of its morphotypes and documenting the range of these morphotypes through the late Middle to Late Eocene in a tropical location.

The studied samples encompassed CNE15–CNO3 and NP17–NP23 (Bartonian–Rupelian), an interval that included the Eocene–Oligocene boundary (E/OB). CNE17–18 and NP18 were missing between 88.02 and 86.85 mbgl due to an unconformity at the contact between the upper Watu Puru Beds and lower Jetis Beds. The Watu Puru Beds (100–88.02 mbgl, totalling 11.98 m) are Bartonian in age, spanning CNE15 (NP16–NP17), and consist of thinly-bedded, silty claystones, interbedded with alternating tuffaceous, andesitic sandstones. The nannofossil preservation varied from moderate in samples with a higher sand content to good in silty clay samples. The Jetis Beds represented the majority of the material examined, ranging from 86.85–41.04 mbgl (totalling 45.81 m), and dated as CNE19 (NP19/20, Priabonian) at the base. All samples comprised silty clays and mudstones, varying from dark to light olive-greens and greys. Between 75.75 and 69.60 mbgl, there was a reddish-brown interval with greenish-grey spots that contained the core's best-preserved nannofossil specimens.

5. Taxonomic discussion

Two species (*Sphenolithus conicus* and *Triquetrorhabdulus carinatus*), which typically appear in the mid- to Late Oligocene (de Kaenel & Villa, 1996; Blaj et al., 2009; Bergen et al., 2017), were identified in the Middle to Upper Eocene sediments of NKK1. This does not appear to be a function of preservation, as both of these species are absent from other Upper Eocene assemblages that have excellent preservation, such as the Tanzanian successions and IODP Expedition 342 in the the North Atlantic Ocean (Bown, 2005; Dunkley Jones et al. 2008, 2009; Bown & Newsam, 2017).

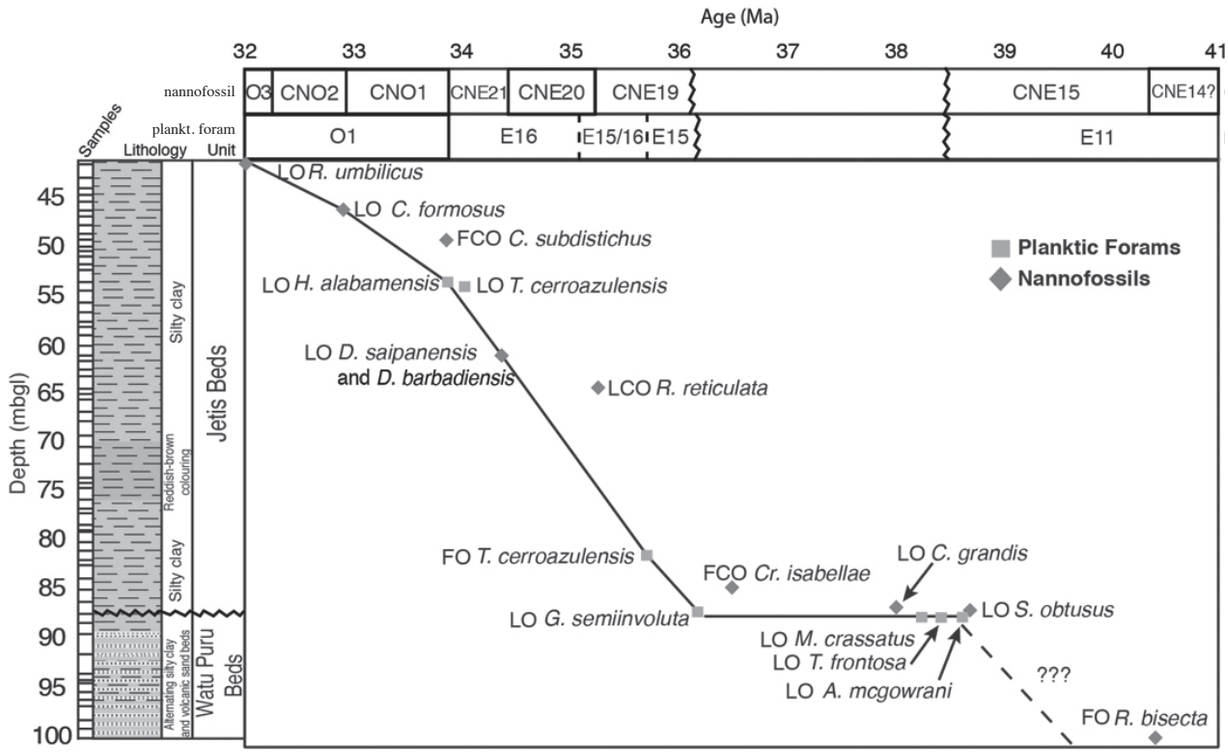

Figure 2: Age/depth plot for NKK1, showing the nannofossil bioevents from Table 1, modified after Jones et al. (2019). Scale and biozones after Agnini et al. (2014). Ages adjusted to the GTS2012 (Gradstein et al., 2012)

Bioevent	Top/Base	Species	Biozone (Martini, 1971)	Biozone (Agnini et al., 2014)	Age (Ma) (Agnini et al., 2014)	Age (Ma) GTS2012 (Gradstein et al., 2012)	Sample ID Bottom	Sample ID Top	Bottom Sample Core Depth (m)	Top Sample Core Depth (m)	Mid-point (m)	Depth Error (±m)
1	top	*Reticulofenestra umbilicus*	NP23	CNO3	32.02	32.02	NKK-1/33a, 43–44	NKK-1/30a, 53–54	45.44	41.04	43.24	2.2
2	top	*Coccolithus formosus*	NP22	CNO2	32.92	32.92	NKK-1/33b, 120–121	NKK-1/33, 43–44	46.21	45.44	45.83	0.39
3	first common occurrence	*Clausicoccus subdistichus*	—	CNO1	33.88	33.86	NKK-1/36a, 43–44	NKK-1/35b, 109–110	49.94	49.1	49.52	0.42
4	top	*Discoaster saipanensis*	NP21	CNE21	34.44	34.37	NKK-1/46a, 55–56	NKK-1/45, 48–49	61.06	59.99	60.53	0.54
5	top	*R. reticulata*	—	CNE20	35.24	35.26	NKK-1/48a, 54–55	NKK-1/47b, 111–112	64.55	63.12	63.84	0.72
6	base	*R. isabellae*	NP19/20	CNE19	36.13	36.49	NKK-1/65, 84–85	NKK-1/64, 23–24	86.85	84.25	85.55	1.3
7	top	*Sphenolithus obtusus*	NP17	CNE16	38.47	38.68	NKK-1/66, 51–52	NKK-1/65, 51–52	88.02	86.85	87.44	0.59
8	base	*R. bisecta*	NP16/17	CNE15	40.34	40.4	NKK-1/>82, 97–98	—	>99.98	—	99.98	—

Table 1: Comparative biostratigraphy of NKK1, using the Agnini et al. (2014) and Martini (1971) biozonation schemes

Sphenolithus conicus is a common mid- to Upper Oligocene species in many pelagic successions (Blaj et al., 2009; Bown & Dunkley Jones, 2012; Bergen et al., 2017). In NKK1, however, *S. conicus* morphotypes appeared in the latest Eocene (Sample NKK1-54a, CNE19, ~35.1 Ma), typically with low abundances that increased into the Lower Oligocene. The *S. conicus* morphotype observed in NKK1 is smaller than the specimens originally described by Bukry (1971), although Bown & Dunkley Jones (2012) also documented a small morphotype in sediments from CNE21 (NP21) from IODP Expedition 320 in the equatorial Pacific. In NKK1, these small *S. conicus* morphotypes are consistently present in assemblages interpreted as CNE19 (NP19/20) (72.44 mbgl, ~35.18 Ma). These specimens are the smallest at the base of their observed range (latest Eocene), increasing in size into the Oligocene (Table 2). *Sphenolithus conicus* first appeared in the IPWP, only later appearing in the East Pacific, suggesting that, in the Early Oligocene, this species was limited to the tropical Pacific.

Triquetrorhabdulus carinatus, a nannolith with uncertain taxonomic affinities, was also present, albeit rarely and sporadically, in CNE19 to CNO3 (NP19/20–NP23, ~35.9 –~31.2 Ma) in the Jetis Beds, although it occurred frequently in Sample NKK1-48a (64.55 mbgl, ~34.7 Ma). Young (1998) and Agnini et al. (2014) stated that the base of *T. carinatus* is in CNO5 (NP25). In our section, it was first observed in CNE19 (NP19/20), approximately 7–8 Myr earlier. Lower Middle Eocene occurrences of *T. carinatus* have been reported from ODP Sites 1209, 1210 and

Reticulofenestra nanggulanensis	Sample ID	Length (μm)	Central-area Width (μm)	Rim Width (μm)	Ratio (Central-area:Rim)	*Sphenolithus conicus*	Sample ID	Height (μm)	Proximal Rim Width (μm)
1	NKK-1/73A, 30–32	6.82	3	1.91	1.57	1	NKK-1/81A, 46–47	4.12	3.53
2	NKK-1/73A, 30–32	6.79	3.22	1.78	1.8	2	NKK-1/81A, 46–47	5.26	4.87
3	NKK-1/73A, 30–32	6.47	2.82	1.82	1.54	3	NKK-1/73A, 30–32	6.53	6.04
4	NKK-1/75, 21–22	5.68	2.77	1.45	1.9	4	NKK-1/73A, 30–32	4.55	4.85
5	NKK-1/75, 21–22	6.44	3.04	1.7	1.78	5	NKK-1/49, 25–26	4.23	3.88
6	NKK-1/80, 73–75	6	2.88	1.56	1.84	6	NKK-1/31A, 40–41	7.81	7.34
7	NKK-1/80, 73–75	5.44	2.49	1.47	1.68	7	NKK-1/31A, 40–41	4.4	4.21
8	NKK-1/80,73–75	5.61	2.71	1.45	1.86	8	NKK-1/30A, 52–54	6.2	4.12
9	NKK-1/81A, 46–47	5.03	2.61	1.21	2.15	9	NKK-1/30A, 52–54	6.34	6.03
10	NKK-1/81A, 46–47	5.02	2.8	1.11	2.52	10	NKK-1/30A, 52–54	6.2	6.9

Table 2: Measurements of *R. nanggulanensis* and *S. conicus* in NKK1

1211, Shatsky Rise, NW Pacific Ocean (Bralower, 2005). Its reported abundances varied from rare to abundant, but there are no figures to accompany these data, and its identification may have been uncertain. There are multiple occurrences of this morphotype in NKK1, in several samples, suggesting that early forms of *T. carinatus* first appeared in the Late Eocene in tropical locations.

Circular reticulofenestrid coccoliths, with distinct central-area nets, are key Middle to Late Eocene taxa, with *R. isabellae* and *R. reticulata* being stratigraphically important (Agnini et al., 2014). They are also palaeoenvironmental markers of relatively warm-water conditions (Bukry, 1973; Aubry, 1992a, b; Newsam et al., 2017). Some authors have placed these forms in the genus *Cribrocentrum* (Fornaciari et al., 2010; Shamrock & Watkins, 2012; Agnini et al., 2014; Self-Trail et al., 2019), but we have retained their placement in the genus *Reticulofenestra*, whilst recognising the same species-level distinctions that are in use. *Reticulofenestra isabellae* was described by Fornaciari et al. (2010) as having large (>12 μm), circular placoliths with a central-area net. These morphotypes are effectively a large variant of *Reticulofenestra reticulata*, which includes medium to large (6–12 μm) coccoliths with a small central-area and distinctive extinction pattern of two crossed 'dumbbells' in the light microscope (LM) (Perch-Nielsen, 1985). *Reticulofenestra erbae* is similar to *R. reticulata*, but has a broad tube and closed central-area (Fornaciari et al., 2010). This morphotype was not seen in NKK1, as its stratigraphic range falls within the unconformity between the Watu Puru and Jetis Beds.

The top of *R. reticulata* is known to be diachronous across latitudes (Berggren et al., 1995), occurring at ~35.32 Ma in the northern mid-latitudes (Agnini et al., 2014), between 36.30 and 36.69 Ma in the southern high latitudes (Villa et al., 2008; Persico et al., 2012) and with a top common occurrence (TCO) at ~34.99 Ma at equatorial Indian Ocean ODP Site 711 (Fioroni et al., 2015). According to Fornaciari et al. (2010), the top of *R. isabellae* is coincident with the top of *R. reticulata* at 35.21 Ma in the Massignano, Zermagnone and Bottaccione sections. This finding is supported by the NKK1 biostratigraphy, where the top of *R. isabellae* coincides with the top of *R. reticulata* at 61.57 mbgl. However, based on the age model for NKK1 (Figure 2), we estimate the synchronous extinctions of *R. reticulata* and *R. isabellae* to be at ~34.5 Ma (CNE20; Figure 3), which is ~0.7–0.8 Myr younger than reported for the northern low to mid-latitudes (Fornaciari et al., 2010; Agnini et al., 2014). Several other Late Eocene tropical nannoplankton have also shown a pattern of continued existence in tropical environments, while being absent from more northerly and southerly regions (Berggren et al., 1995; Dunkley Jones et al., 2008; Fioroni et al., 2015). The co-extinction of these two morphotypes in NKK1 and at other locations (Fornaciari et al., 2010) poses the question whether separating the two species, based on a 12 μm size difference, is an arbitrary division of a population with continuous size variability. However, the limited age range of the large morphotype may still have biostratigraphic utility in the Upper Eocene (Agnini et al., 2014).

Reticulofenestra nanggulanensis sp. nov. is distinguished from *R. reticulata* by its characteristically wide central-area, and from *R. lockeri* by its subcircular shape (Plate 1, figs 40–42). *Reticulofenestra nanggulanensis* is medium in size (5–7 μm), with a single, slim outer cycle, and lacks the inner cycle that is present in *R. reticulata* and *R. isabellae*. This morphotype has been illustrated previously by Bown & Newsam (2017; Plate 2, figs 7–9) as *R. reticulata* (wide). This new species is not only distinct, but also has a different stratigraphic range from *R. reticulata*.

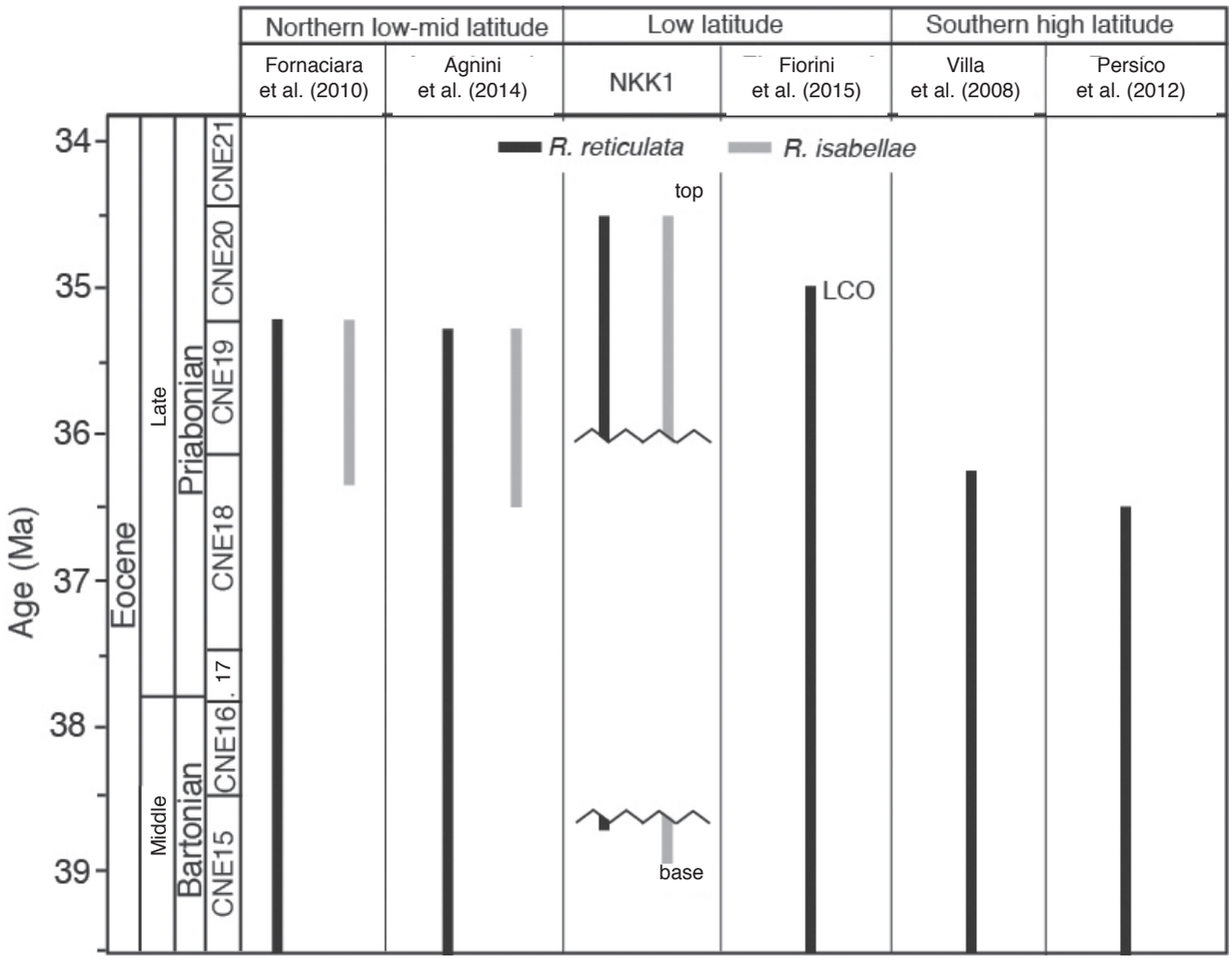

Figure 3: Stratigraphic distribution of *R. reticulata* and *R. isabellae*, showing diachroneity in the occurrences of these species across different latitudes. The northern, low- to mid-latitude data are from IODP Site 1218, ODP Sites 1051 and 1052, the Cicogna and Possagno sections and the Mediterranean area (Fornaciari et al., 2010; Agnini et al., 2014). The equatorial low-latitude data are from NKK1 (this study) and ODP Site 711 (Fioroni et al., 2015). DSDP Site 522 and IODP Site 1262 give the southern mid-latitude data (Fornaciari et al., 2010; Agnini et al., 2014). The southern high-latitude data are from ODP Holes 784B (Villa et al., 2008) and 689D (Persico et al., 2012). Ages for the occurrences of *R. reticulata* and *R. isabellae* have been recalibrated against the GTS2012 (Gradstein et al., 2012)

It occurs in stratigraphically older sediments, in CNE15 (NP16/17, 99.98–88.86 mbgl), and with rare abundances above the extinction of *R. reticulata*, up to CNO1 (NP21, 46.21 mbgl) in the Lower Oligocene. Once *R. reticulata* appears in the section (88.86 mbgl), the abundance of *R. nanggulanensis* decreases, although it occurs consistently in all samples up to the end of CNE19 (NP19/20, 64.55 mbgl), and then continues as rare occurrences into the lowest Oligocene.

The recognition of species of *Calcidiscus* throughout the Palaeogene is growing (Bown et al., 2007; Dunkley Jones et al., 2009; Bown & Dunkley Jones, 2012; da Gama & Varol, 2014). Calcidiscids are present, although not particularly diverse, in NKK1, but two species were recognised—*C. bicircus* and *C.* cf. *C. gallagheri* (Plate 3, figs 9–11, Plate 3, figs 14–17). It is possible that additional species are present in the oldest section of the core, but the poor preservation of central-area structures in these samples makes this equivocal. From DSDP Leg 25 Site 242 in the western Indian Ocean, along the Davis Ridge, da Gama & Varol (2014) described one new species—*C. gallagheri*—from CNO5 (NP25). We recorded the occurrence of a specimen similar to *C. gallagheri* in the Upper Eocene. The base of *C.* cf. *C. gallagheri* in the NKK1 core was found in CNE19 (NP19/20), above which, this species became progressively more common into the lowest Oligocene (64.55–41.04 mbgl).

A new species of *Coccolithus*—*C. aspida* (Plate 2, figs 1, 2)—is described from NKK1. The morphological variation in the genus *Coccolithus* in the NKK1 assemblages was high, in terms of both size and central-area structure. Closely-coupled genetic and morphological variation in

modern *Coccolithus* species (Narciso et al., 2006) supports a robust differentiation among species based on subtle morphological differences. *Coccolithus aspida* is clearly distinct from *C. pelagicus* due to its closed central-area and broad outer rim, and it is persistently common throughout NKK1. *Coccolithus pelagicus* and its morphotypes all have an open central-area, some spanned by bars and crosses, but this is the first species to be described with a fully-closed central-area.

Overall, application of the Agnini et al. (2014) biozonation scheme to the NKK1 data worked well, whilst using both Agnini et al. (2014) and Martini (1971) improves the stratigraphic subdivision of the Upper Eocene, with more nannofossil biohorizons being identified at low- and low-mid-latitude locations. The calibrated ages of Late Eocene bioevents from Agnini et al. (2014) provided a coherent age model for NKK1, and are highly consistent with the bioevent ages from planktonic foraminifera. The only problematic datum was the top of *R. reticulata*, which was offset from the general age-depth trend defined by the nannofossil and planktonic foraminiferal age constraints (Figure 2). Based on the age model for NKK1, we estimate that the top of *R. reticulata* was ~0.7–0.8 Myr younger in NKK1 than was estimated by Agnini et al. (2014), supporting previous indications for latitudinal diachroneity of this event (Berggren et al., 1995). The Middle and Middle –Upper Eocene biostratigraphy of NKK1 was complicated by the unconformity between the upper Watu Puru Beds and lower Jetis Beds (88.02–86.85 mbgl), which spanned CNE17–CNE18 and NP18. As a result, the boundary between the Middle and Upper Eocene was not present in the section, and it was thus not possible to assess the applicability of these zones in this study.

6. Systematic palaeontology

Images of some of the nannofossils found in NKK1 are presented in six plates. These plates display the diversity and morphological variation of species recorded from the upper Middle Eocene to Lower Oligocene. The descriptive terminology below follows Young et al. (1997), and the higher taxonomic classification is based on Young & Bown (1997) for extinct taxa and Young et al. (2003) for extant taxa. We aimed to make the taxonomy consistent with recent, extensive systematic studies of Palaeogene calcareous nannofossils (Bown, 2005; Bown et al., 2007; Dunkley Jones et al., 2009; Bown & Dunkley Jones, 2012; Bown & Newsam, 2017). Our taxonomic comments only pertain to taxa with particular significance, species where our taxonomic concepts diverge from, or are a clarification of, those previously published, or are descriptions of the two new species.

The sample identifications on the plates use a 'core, section (A or B) and interval-in-section (cm)' notation. Where an image is a rotation of the same specimen as the preceding image, the sample information is not replicated. Additionally, the name of a specimen is not replicated when it is of the same species. All images were taken at the same magnification.

6.1 Placolith coccoliths

Order ISOCHRYSIDALES Paascher, 1910
Family NOELAERHABDACEAE Jerkovic, 1970
emend. Young & Bown, 1997

Cyclicargolithus floridanus group
Pl. 1, figs 8–10

Description: Small to large, subcircular to broadly elliptical reticulofenestrids displaying a narrow central-area and indiscernible net (which may be missing or non-birefringent).

Cyclicargolithus floridanus (Roth & Hay *in* Hay et al., 1967) Bukry, 1971
Pl. 1, figs 9, 10

Remarks: All small to large (3–11 μm), subcircular reticulofenestrids possessing a narrow central-area. Specimens with a closed central-area were here placed in *C.* cf. *C. floridanus*.

Cyclicargolithus cf. *C. floridanus* (Roth & Hay *in* Hay et al., 1967) Bukry, 1971
Pl. 1, fig. 8

Remarks: *C. floridanus* with a closed central-area.

Reticulofenestra bisecta group
Pl. 1, figs 20, 21, 31–34

Description: *Reticulofenestra*s (*Dictyococcites* of some authors) with a central-area that is birefringent, and

Plate 1

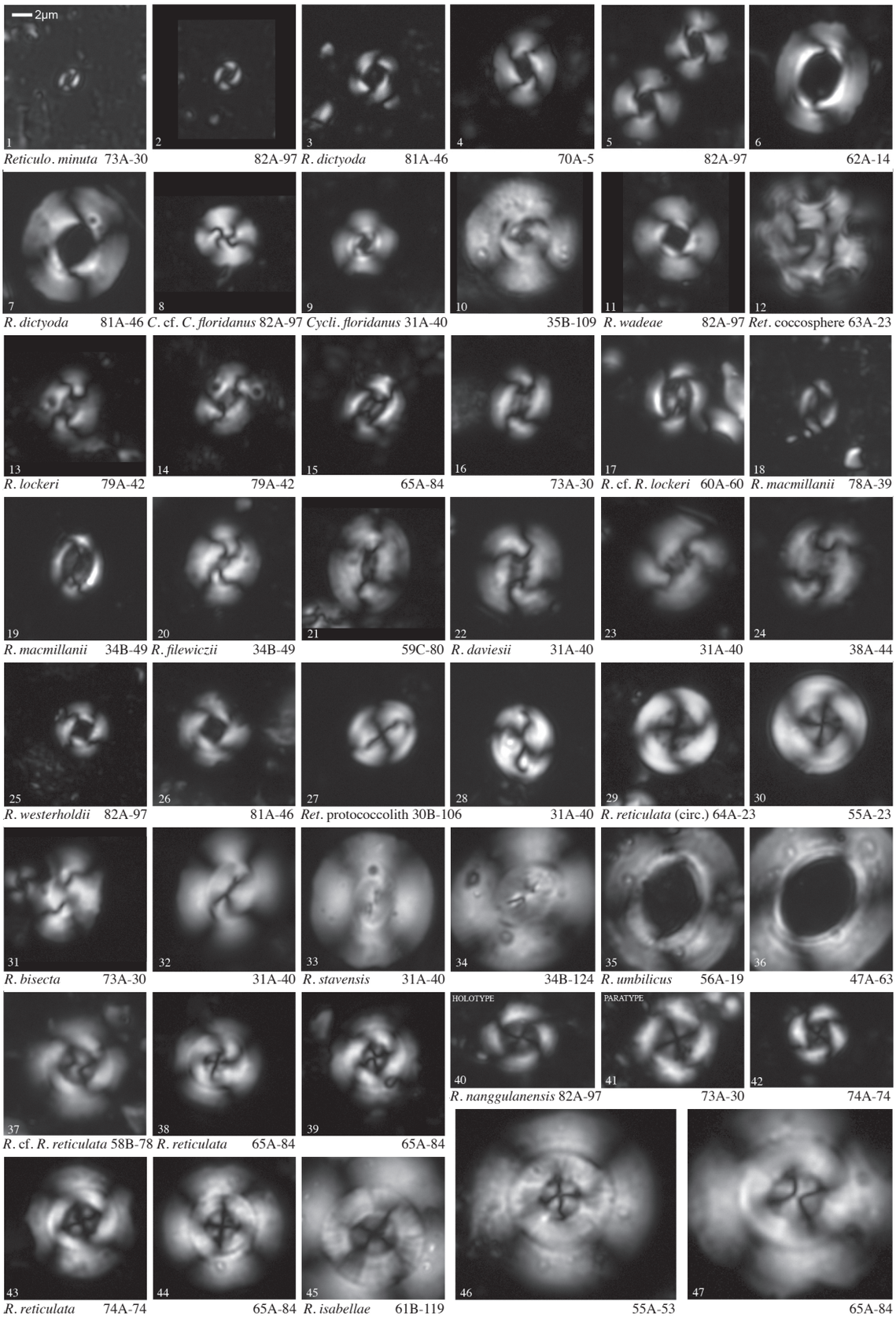

Reticulo. minuta 73A-30 82A-97 *R. dictyoda* 81A-46 70A-5 82A-97 62A-14

R. dictyoda 81A-46 *C.* cf. *C. floridanus* 82A-97 *Cycli. floridanus* 31A-40 35B-109 *R. wadeae* 82A-97 *Ret.* coccosphere 63A-23

R. lockeri 79A-42 79A-42 65A-84 73A-30 *R.* cf. *R. lockeri* 60A-60 *R. macmillanii* 78A-39

R. macmillanii 34B-49 *R. filewiczii* 34B-49 59C-80 *R. daviesii* 31A-40 31A-40 38A-44

R. westerholdii 82A-97 81A-46 *Ret.* protococcolith 30B-106 31A-40 *R. reticulata* (circ.) 64A-23 55A-23

R. bisecta 73A-30 31A-40 *R. stavensis* 31A-40 34B-124 *R. umbilicus* 56A-19 47A-63

R. nanggulanensis 82A-97 73A-30 74A-74

R. cf. *R. reticulata* 58B-78 *R. reticulata* 65A-84 65A-84

R. reticulata 74A-74 65A-84 *R. isabellae* 61B-119 55A-53 65A-84

closed by a distinct plug. Included species: *R. bisecta* (*D. scrippsiae*), *R. filewiczii*, *R. stavensis* (*D. bisectus*).

Reticulofenestra bisecta (Hay et al., 1966) Roth, 1970
Pl. 1, figs 31, 32

Remarks: Elliptical and medium to large (less than 10 μm long), with a solid plug.

Reticulofenestra filewiczii (Wise & Wiegand *in* Wise, 1983) Dunkley Jones et al., 2009
Pl. 1, figs 20, 21

Remarks: Differs from the rest of the group in having a small central opening and weakly birefringent net.

Reticulofenestra stavensis (Levin & Joerger, 1967) Varol, 1989
Pl. 1, figs 33, 34

Remarks: Similar morphology to *R. bisecta*, but distinguished by its larger size (>10 μm).

Reticulofenestra lockeri group
Pl. 1, figs 13–19, 22–24

Description: Elliptical reticulofenestrids with a visible (birefringent) net, with perforations that are sometimes discernible in the LM. Included species: *R. daviesii*, *R. lockeri*, *R.* cf. *R. lockeri*, *R. macmillanii*.

Reticulofenestra daviesii (Haq, 1968) Haq, 1971
Pl. 1, figs 22–24

Remarks: Differentiated from *R. lockeri* by the single row of perforations on each side of the netted central-area. The species became more common above the E/OB, but was sporadic throughout the section.

Reticulofenestra lockeri Müller, 1970
Pl. 1, figs 13–16

Remarks: Elliptical, with a visible central-area net that has no perforations observable in the LM. The central-area is narrow; those with wider central-areas were placed in *R.* cf. *R. lockeri*.

Reticulofenestra cf. *R. lockeri* Müller, 1970
Pl. 1, fig. 17

Remarks: Similar to *R. lockeri*, but with a wider central-area that has a visible (birefringent) net.

Reticulofenestra macmillanii Dunkley Jones et al., 2009
Pl. 1, figs 18, 19

Remarks: Similar to *R. lockeri*, but smaller, and with a wider central-area.

Reticulofenestra reticulata group
Pl. 1, figs 25, 26, 37–47

Description: Medium to very large, circular reticulofenestrids with a circular to broadly-elliptical central-area, spanned by a robust and conspicuous (birefringent) net. Included species: *R. isabellae*, *R. nanggulanensis*, *R. reticulata*, *R.* cf. *R. reticulata*, *R. westerholdii*.

Reticulofenestra isabellae (Catanzariti et al. *in* Fornaciari et al., 2010) Bown & Newsam, 2017
Pl. 1, figs 45–47

Remarks: Very large reticulofenestrid (>12 μm), with a relatively narrow central-area and broad tube-cycle. **Occurrence**: CNE16–CNE20, NP17–NP19/20.

Reticulofenestra nanggulanensis sp. nov.
Pl. 1, figs 40–42

Derivation of name: After the Nanggulan Formation in south-central Java, the geological formation from which the NKK1 samples originated. **Diagnosis**: Small to medium, subcircular reticulofenestrid, with a distinct, wide central-area (>1.5 times the rim width). The central-area is spanned by a visible (birefringent) net. **Differentiation**: Similar to *R. reticulata*, but has only one outer shield and a distinctly wider central-area, which varies from broadly elliptical to subcircular. **Remarks**: Most common in CNE15 (NP17), and more common than other members of the *R. reticulata* group in this core. Consistently observed up to the top of CNE19 (NP19/20), and present to the top of CNO1 (NP21). **Dimensions**: Holotype length = 6.0 μm; paratype length = 7.2 μm. **Holotype**: Plate 1, fig. 40.

Plate 2

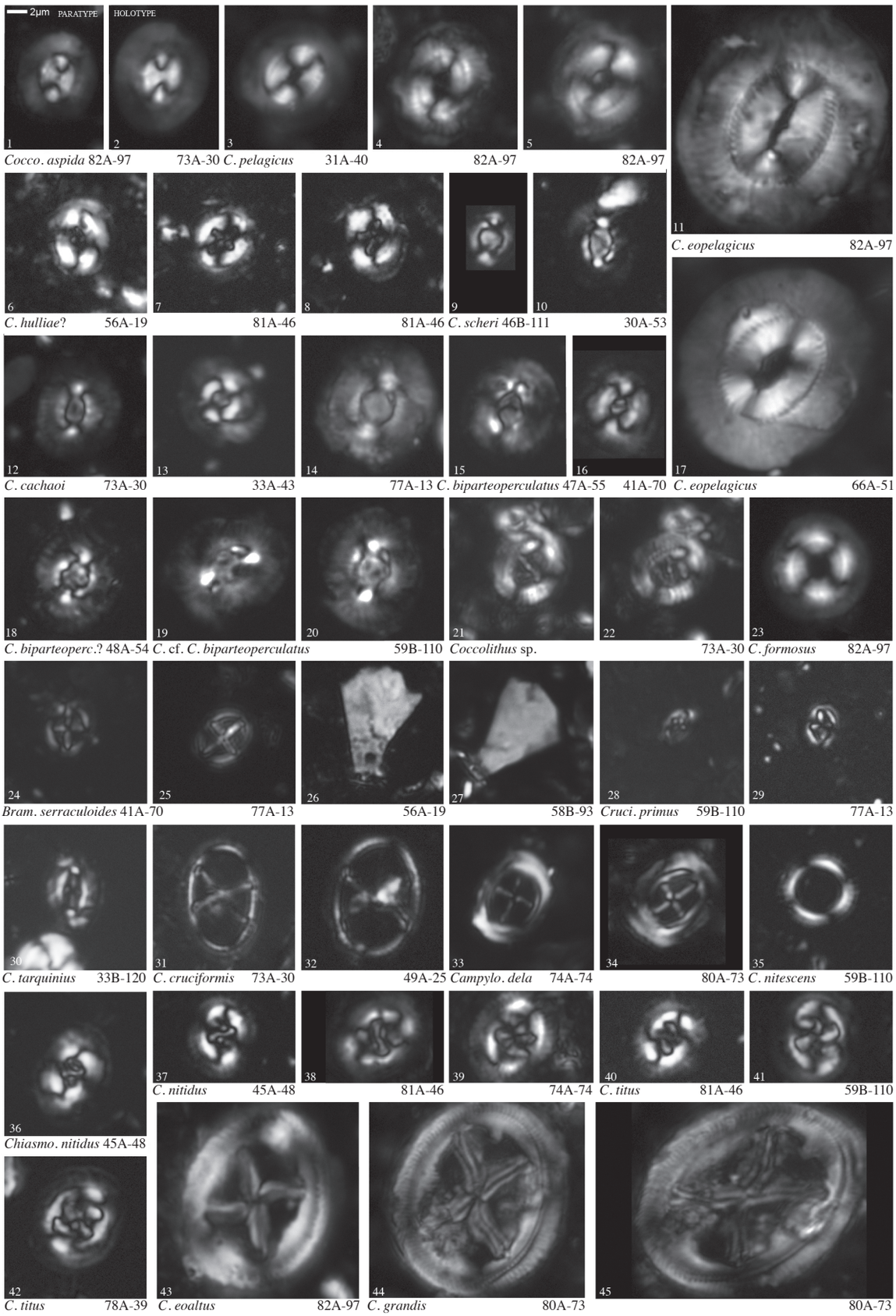

Cocco. aspida 82A-97 73A-30 *C. pelagicus* 31A-40 82A-97 82A-97

C. eopelagicus 82A-97

C. hulliae? 56A-19 81A-46 81A-46 *C. scheri* 46B-111 30A-53

C. cachaoi 73A-30 33A-43 77A-13 *C. biparteoperculatus* 47A-55 41A-70 *C. eopelagicus* 66A-51

C. biparteoperc.? 48A-54 *C.* cf. *C. biparteoperculatus* 59B-110 *Coccolithus* sp. 73A-30 *C. formosus* 82A-97

Bram. serraculoides 41A-70 77A-13 56A-19 58B-93 *Cruci. primus* 59B-110 77A-13

C. tarquinius 33B-120 *C. cruciformis* 73A-30 49A-25 *Campylo. dela* 74A-74 80A-73 *C. nitescens* 59B-110

C. nitidus 45A-48 81A-46 74A-74 *C. titus* 81A-46 59B-110

Chiasmo. nitidus 45A-48

C. titus 78A-39 *C. eoaltus* 82A-97 *C. grandis* 80A-73 80A-73

Paratype: Plate 1, fig. 41. **Type locality**: NKK1, Nanggulan, Java. **Type level**: Upper Middle Eocene, NKK1-82A-97cm, CNE15, NP17. **Occurrence**: Recorded in upper Middle Eocene to Lower Oligocene sediments, CNE15–CNO1, NP16–NP17. Top recorded in sample NKK1-33b (46.21 mbgl).

Reticulofenestra reticulata (Gartner & Smith, 1967) Roth & Thierstein, 1972
Pl. 1, figs 38, 39, 43, 44

Remarks: Used broadly for medium to large (<12 μm), circular reticulofenestrids, with a broad tube-cycle and narrow central-area having a visible (birefringent) net.

Reticulofenestra cf. *R. reticulata* (Gartner & Smith, 1967) Roth & Thierstein, 1972
Pl. 1, fig. 37

Remarks: Similar to *R. reticulata*, but with a larger central-area. This form has two distinct cycles and, therefore, is not *R. nanggulanensis*.

Reticulofenestra reticulata (circular) (Gartner & Smith, 1967) Roth & Thierstein, 1972
Pl. 1, figs 28–30

Remarks: Similar to *R. reticulata*, but circular rather than having the common broadly-elliptical shape.

Reticulofenestra westerholdii Bown & Dunkley Jones, 2012
Pl. 1, figs 25, 26

Remarks: Circular, with a central-area net that is not visible in the LM. Morphologically very similar to other members of the *R. reticulata* group.

Reticulofenestra umbilicus group
Pl. 1, figs 1–7, 11, 35, 36

Description: Elliptical and subcircular reticulofenestrids with an open central-area, spanned by a thin, faint (non-birefringent or missing) net. Included species: *R. dictyoda*, *R. minuta*, *R. umbilicus*, *R. wadeae*.

Reticulofenestra dictyoda (Deflandre *in* Deflandre & Fert, 1954) Stradner *in* Stradner & Edwards, 1968
Pl. 1, figs 3–7

Remarks: Used broadly to distinguish medium to large, elliptical reticulofenestrids, with relatively-open central-areas.

Reticulofenestra minuta Roth, 1970
Pl. 1, figs 1, 2

Remarks: Used broadly here for elliptical reticulofenestrids that are very small (<3 μm).

Reticulofenestra umbilicus (Levin, 1965) Martini & Ritzkowski, 1968
Pl. 1, figs 35, 36

Remarks: Very large (>14 μm), elliptical reticulofenestrid.

Reticulofenestra wadeae Bown, 2005
Pl. 1, fig. 11

Order COCCOLITHALES Haeckel, 1894 emend. Young & Bown, 1997
Family COCCOLITHACEAE Poche, 1913 emend. Young & Bown, 1997

Coccolithus pelagicus group
Pl. 2, figs 1–5, 11, 17, 21, 22

Description: Elliptical to subcircular *Coccolithus*es, with a central opening sometimes having a delicate bar or cross.

Coccolithus aspida sp. nov.
Pl. 2, figs 1, 2

Derivation of name: From the Greek '*aspída*', meaning 'shield', referring to the distinctive *Coccolithus*-type outer rim. **Diagnosis**: Medium to large, elliptical *Coccolithus*, with a noticeable V-unit-dominated outer rim that is larger than the tube-cycle and possesses an apparently-closed central-area. **Differentiation**: Distinguished from *C. pelagicus* by its closed central-area. **Remarks**: This species occurred commonly in all the samples from NKK1. Al-

Plate 3

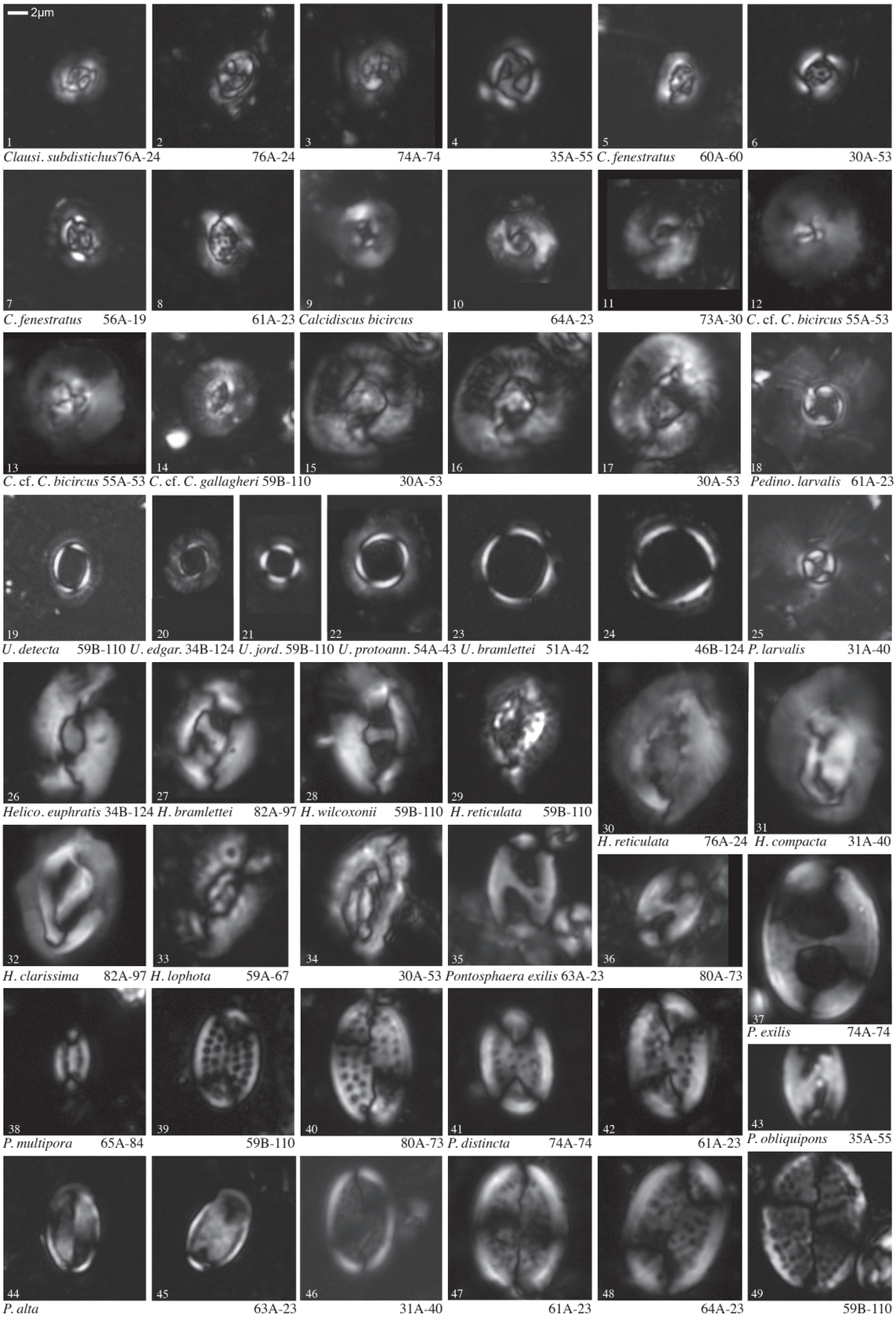
2µm
1 Clausi. subdistichus 76A-24
2 76A-24
3 74A-74
4 35A-55
5 C. fenestratus 60A-60
6 30A-53
7 C. fenestratus 56A-19
8 61A-23
9 Calcidiscus bicircus 64A-23
10
11 73A-30
12 C. cf. C. bicircus 55A-53
13 C. cf. C. bicircus 55A-53
14 C. cf. C. gallagheri 59B-110
15 30A-53
16
17 30A-53
18 Pedino. larvalis 61A-23
19 U. detecta 59B-110
20 U. edgar. 34B-124
21 U. jord. 59B-110
22 U. protoann. 54A-43
23 U. bramlettei 51A-42
24 46B-124
25 P. larvalis 31A-40
26 Helico. euphratis 34B-124
27 H. bramlettei 82A-97
28 H. wilcoxonii 59B-110
29 H. reticulata 59B-110
30 H. reticulata 76A-24
31 H. compacta 31A-40
32 H. clarissima 82A-97
33 H. lophota 59A-67
34 30A-53
35 Pontosphaera exilis 63A-23
36 80A-73
37 P. exilis 74A-74
38 P. multipora 65A-84
39 59B-110
40 80A-73
41 P. distincta 74A-74
42 61A-23
43 P. obliquipons 35A-55
44 P. alta
45 63A-23
46 31A-40
47 61A-23
48 64A-23
49 59B-110

though this species is characterised by a closed central-area, its overall morphology and crystallography are very similar to those of *C. pelagicus*, and so we have placed the new species in *Coccolithus*, pending further observations of this morphotype. In the future, the generic description of *Coccolithus* (having an open central-area) may need to be emended. **Dimensions**: Holotype length = 10.8 μm, paratype length = 8.1 μm. **Holotype**: Plate 2, fig. 2. **Paratype**: Plate 2, fig. 1. **Type locality**: NKK1, Nanggulan, Java. **Type level**: Middle Eocene, Sample NKK1-73A-30cm, CNE15, NP17. **Occurrence**: Recorded in Middle Eocene to Lower Oligocene sediments, CNE15–CNO3, NP16–NP23.

Coccolithus eopelagicus (Bramlette & Riedel, 1954)
Bramlette & Sullivan, 1961
Pl. 2, figs 11, 17

Coccolithus sp.
Pl. 2, figs 21, 22

Description: Large and broadly elliptical *Coccolithus*-type coccolith, with a broad rim and a delicate, disjunct, transverse bar that spans the open central-area and has a small nodule in the centre. The bar curves slightly at each end when the ellipse is aligned at 0°. When rotated to 45°, the transverse bar becomes a thin, dark 'S'-shape, similar to that of *Chiasmolithus titus*, although *C. titus* is otherwise distinctly dissimilar. **Remarks**: Only one specimen was recorded, in NKK1-73A-30cm, CNE15, NP16/17, Middle Eocene.

Coccolithus pelagicus (Wallich, 1877) Schiller, 1930
Pl. 2, figs 3–5

Coccolithus biparteoperculatus group
Pl. 2, figs 9, 10, 12–16, 18–20

Description: The central-area, which can be broad or netted, is filled by a bar.

Coccolithus biparteoperculatus (Varol, 1991)
Bown & Dunkley Jones, 2012
Pl. 2, figs 15, 16, 18

Coccolithus cf. *C. biparteoperculatus*
Pl. 2, figs 19, 20

Remarks: Similar to *C. biparteoperculatus*, but the bipartite, oval bar appears perforated, making it look like a net or grill, which may be the result of overcalcification.

Coccolithus cachaoi Bown, 2005
Pl. 2, figs 12–14

Coccolithus scheri Bown & Dunkley Jones, 2012
Pl. 2, figs 9, 10

Other *Coccolithus* species

Coccolithus formosus (Kamptner, 1963) Wise, 1973
Pl. 2, fig. 23

Coccolithus hulliae? Bown & Newsam, 2017
Pl. 2, figs 6–8

Remarks: Questionable assignment because the central-area cross is different from that described by Bown & Newsam (2017). As pictured in Plate 2, *C. hulliae*? has a disjunct axial cross that intersects the inner cycle. However, the rim morphology is similar to that described by Bown & Newsam (2017).

Chiasmolithus bidens group
Pl. 2, figs 43–45

Chiasmolithus eoaltus Persico & Villa, 2008
Pl. 2, fig. 43

Chiasmolithus grandis (Bramlette & Riedel, 1954)
Radomski, 1968
Pl. 2, figs 44, 45

Remarks: This species was recorded from the base of the core, although its presence was rare. However, an acme of *C. grandis* was observed in one sample (NKK-1/66, 51–52), just below the unconformity between 88.02 and 86.85 mbgl.

Plate 4

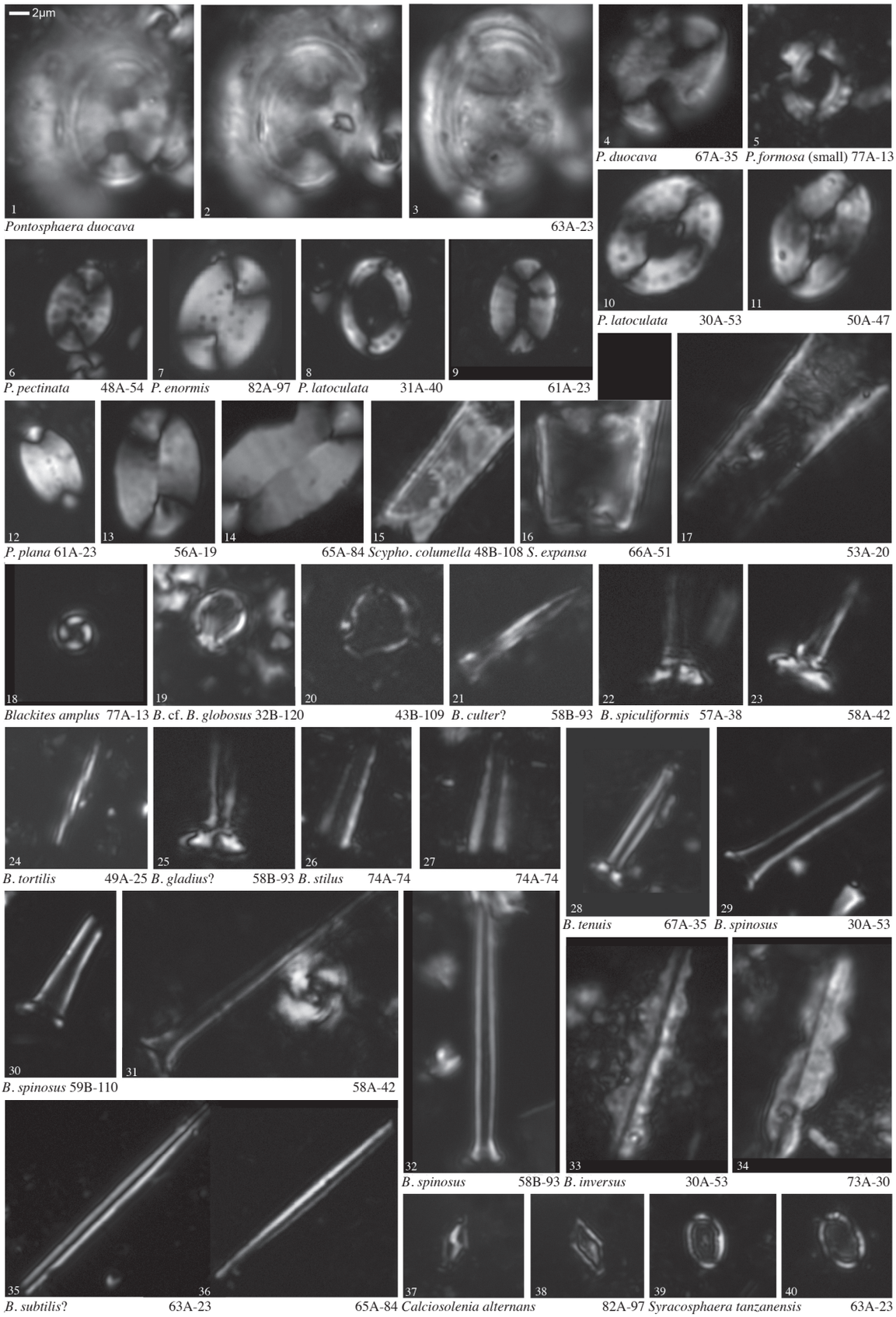

Pontosphaera duocava 63A-23

P. duocava 67A-35 *P. formosa* (small) 77A-13

P. latoculata 30A-53 50A-47

P. pectinata 48A-54 *P. enormis* 82A-97 *P. latoculata* 31A-40 61A-23

P. plana 61A-23 56A-19 65A-84 *Scypho. columella* 48B-108 *S. expansa* 66A-51 53A-20

Blackites amplus 77A-13 *B.* cf. *B. globosus* 32B-120 43B-109 *B. culter*? 58B-93 *B. spiculiformis* 57A-38 58A-42

B. tortilis 49A-25 *B. gladius*? 58B-93 *B. stilus* 74A-74 74A-74

B. tenuis 67A-35 *B. spinosus* 30A-53

B. spinosus 59B-110 58A-42

B. spinosus 58B-93 *B. inversus* 30A-53 73A-30

B. subtilis? 63A-23 65A-84 *Calciosolenia alternans* 82A-97 *Syracosphaera tanzanensis* 63A-23

Chiasmolithus consuetus group
Pl. 2, figs 36–42

Chiasmolithus nitidus Perch-Nielsen, 1971
Pl. 2, figs 36–39

Chiasmolithus titus Gartner, 1970
Pl. 2, figs 40–42

Campylosphaera–Cruciplacolithus group
Pl. 2, figs 24–34

Bramletteius serraculoides Gartner, 1969
Pl. 2, figs 24–27

Campylosphaera dela (Bramlette & Sullivan, 1961) Hay & Mohler, 1967
Pl. 2, figs 33, 34

Cruciplacolithus cruciformis (Hay & Towe, 1962) Roth, 1970
Pl. 2, figs 31, 32

Cruciplacolithus primus Perch-Nielsen, 1977
Pl. 2, figs 28, 29

Description: Small, elliptical *Cruciplacolithus*, with a disjunct, axial cross in the central-area. Very narrow, bicyclic rim.

Cruciplacolithus tarquinius Roth & Hay *in* Hay et al., 1967
Pl. 2, fig. 30

Description: Narrowly elliptical, and small to medium in size. The central-area contains a small, delicate axial cross. The rim is bicyclic, and broader than that of *C. primus*.

Clausicoccus group
Clausicoccus fenestratus (Deflandre & Fert, 1954) Prins, 1979
Pl. 3, figs 5–8

Clausicoccus subdistichus (Roth & Hay *in* Hay et al., 1967) Prins, 1979
Pl. 3, figs 1–4

Coronocyclus group
Coronocyclus nitescens (Kamptner, 1963) Bramlette & Wilcoxon, 1967
Pl. 2, fig. 35

Family CALCIDISCACEAE Young & Bown, 1997

Calcidiscus bicircus Bown, 2005
Pl. 3, figs 9–11

Calcidiscus cf. *C. bicircus* Bown, 2005
Pl. 3, figs 12, 13

Remarks: Similar to *C. bicircus*, but with a closed central-area and visible (birefringent) net.

Calcidiscus cf. *C. gallagheri* da Gama & Varol, 2014
Pl. 3, figs 14–17

Description: Broadly elliptical, medium to very large. The central-area is distinctive, with a delicate net (partially missing in both specimens) and small perforations visible in the LM. **Remarks**: The central-area is more irregular than that described by da Gama & Varol (2014); this specimen appears to be more heavily calcified, despite being of a similar size and shape.

Umbilicosphaera bramlettei (Hay & Towe, 1962) Bown et al., 2007
Pl. 3, figs 23, 24

Remarks: A variation in size was documented in the Upper Eocene through Lower Oligocene of NKK1. Larger specimens (>8 μm) occurred in the lower Upper Eocene (CNE19, NP19/20).

Umbilicosphaera detecta (de Kaenel & Villa, 1996) Young & Bown, 2014
Pl. 3, fig. 19

Umbilicosphaera edgariae (Bown & Dunkley Jones, 2012) Young & Bown, 2014
Pl. 3, fig. 20

Umbilicosphaera jordanii Bown, 2005
Pl. 3, fig. 21

Plate 5

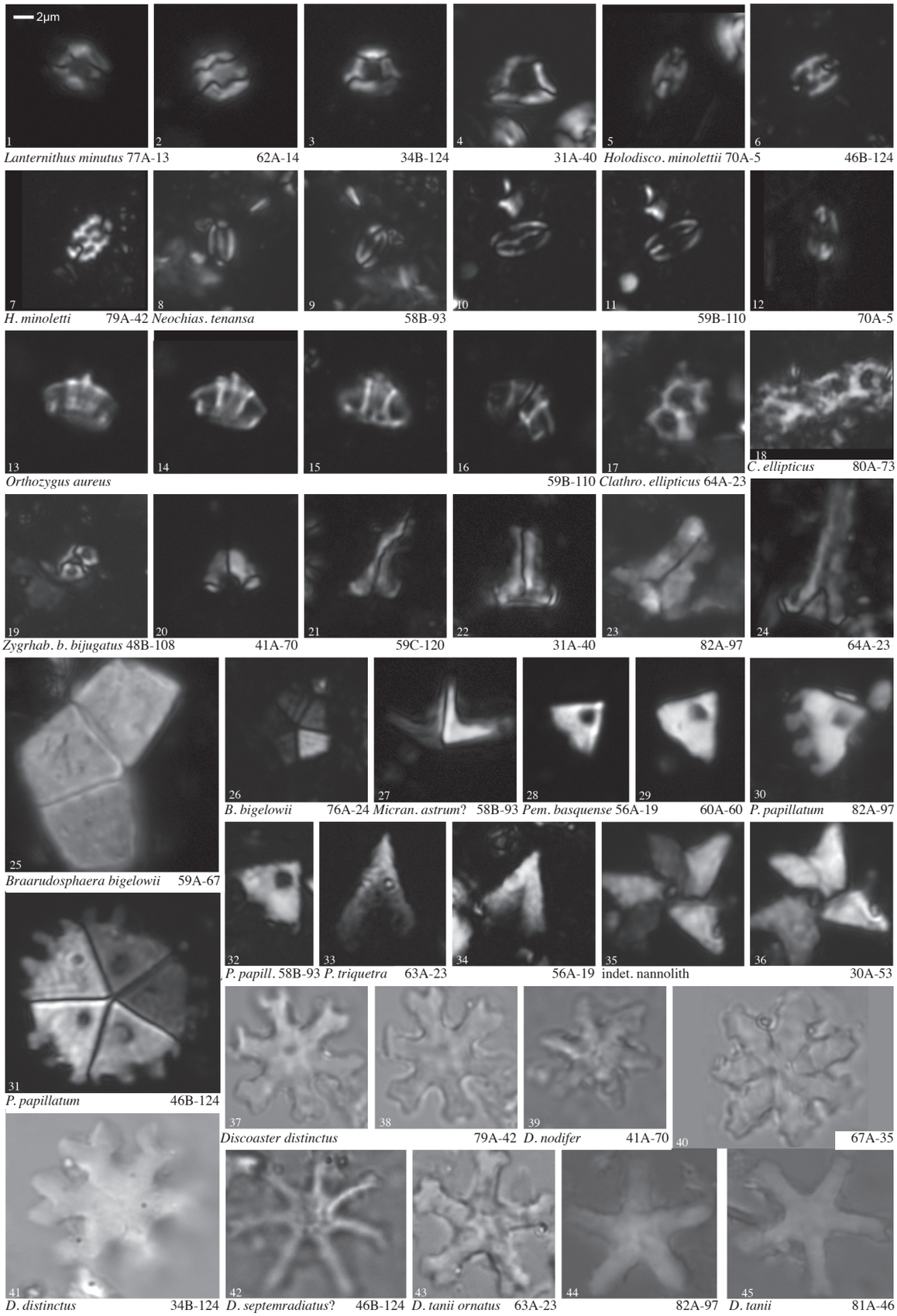
2µm
1
2
3
4
5
6
Lanternithus minutus 77A-13
62A-14
34B-124
31A-40
Holodisco. minolettii 70A-5
46B-124
7
8
9
10
11
12
H. minoletti 79A-42
Neochias. tenansa 58B-93
59B-110
70A-5
13
14
15
16
17
18
Orthozygus aureus
59B-110
Clathro. ellipticus 64A-23
C. ellipticus 80A-73
19
20
21
22
23
24
Zygrhab. b. bijugatus 48B-108
41A-70
59C-120
31A-40
82A-97
64A-23
25
26
27
28
29
30
Braarudosphaera bigelowii 59A-67
B. bigelowii 76A-24
Micran. astrum? 58B-93
Pem. basquense 56A-19
60A-60
P. papillatum 82A-97
31
32
33
34
35
36
P. papillatum 46B-124
P. papill. 58B-93
P. triquetra 63A-23
56A-19
indet. nannolith
30A-53
37
38
39
40
Discoaster distinctus 79A-42
D. nodifer 41A-70
67A-35
41
42
43
44
45
D. distinctus 34B-124
D. septemradiatus? 46B-124
D. tanii ornatus 63A-23
82A-97
D. tanii 81A-46

Umbilicosphaera protoannulus (Gartner, 1971)
Young & Bown, 2014
Pl. 3, fig. 22

Placolith coccoliths incertae sedis

Pedinocyclus larvalis (Bukry & Bramlette, 1969)
Loeblich & Tappan, 1973
Pl. 3, figs 18, 25

6.2 Murolith Coccoliths

Order ZYGODISCALES Young & Bown, 1997
Family HELICOSPHAERACEAE Black, 1971

Helicosphaera bramlettei (Müller, 1970)
Jafar & Martini, 1975
Pl. 3, fig. 27

Helicosphaera clarissima Bown, 2005
Pl. 3, fig. 32

Helicosphaera compacta Bramlette & Wilcoxon, 1967
Pl. 3, fig. 31

Helicosphaera euphratis Haq, 1966
Pl. 3, fig. 26

Helicosphaera lophota (Bramlette & Sullivan, 1961)
Locker, 1973
Pl. 3, figs 33, 34

Helicosphaera reticulata Bramlette & Wilcoxon, 1967
Pl. 3, figs 29, 30

Helicosphaera wilcoxonii (Gartner, 1971)
Jafar & Martini, 1975
Pl. 3, fig. 28

Family PONTOSPHAERACEAE Lemmermann, 1908

Pontosphaera alta Roth, 1970
Pl. 3, figs 44–49

Pontosphaera distincta (Bramlette & Sullivan, 1961)
Roth & Thierstein, 1972
Pl. 3, figs 41, 42

Pontosphaera duocava (Bramlette & Sullivan, 1961)
Romein, 1979
Pl. 4, figs 1–4

Pontosphaera enormis (Locker, 1967)
Perch-Nielsen, 1984
Pl. 4, fig. 7

Pontosphaera exilis (Bramlette & Sullivan, 1961)
Romein, 1979
Pl. 3, figs 35–37

Pontosphaera formosa (Bukry & Bramlette, 1969)
Romein, 1979
Pl. 4, fig. 5

Remarks: Our forms were smaller than the originally-described size of 14–17 μm (Romein, 1979).

Pontosphaera latoculata (Bukry & Percival, 1971)
Perch-Nielsen, 1984
Pl. 4, figs 8–11

Remarks: This species exhibited a wide variation in rim thickness. It also had a single cycle of perforations around the rim and an open central-area that varied in width.

Pontosphaera multipora (Kamptner, 1948 ex Deflandre *in* Deflandre & Fert, 1954) Roth, 1970
Pl. 3, figs 38–40

Pontosphaera pectinata (Bramlette & Sullivan, 1961)
Sherwood, 1974
Pl. 4, fig. 6

Pontosphaera plana (Bramlette & Sullivan, 1961)
Haq, 1971
Pl. 4, figs 12–14

Pontosphaera obliquipons (Deflandre *in* Deflandre & Fert, 1954) Romein, 1979
Pl. 3, fig. 43

Scyphosphaera columella Stradner, 1969
Pl. 4, fig. 15

Plate 6

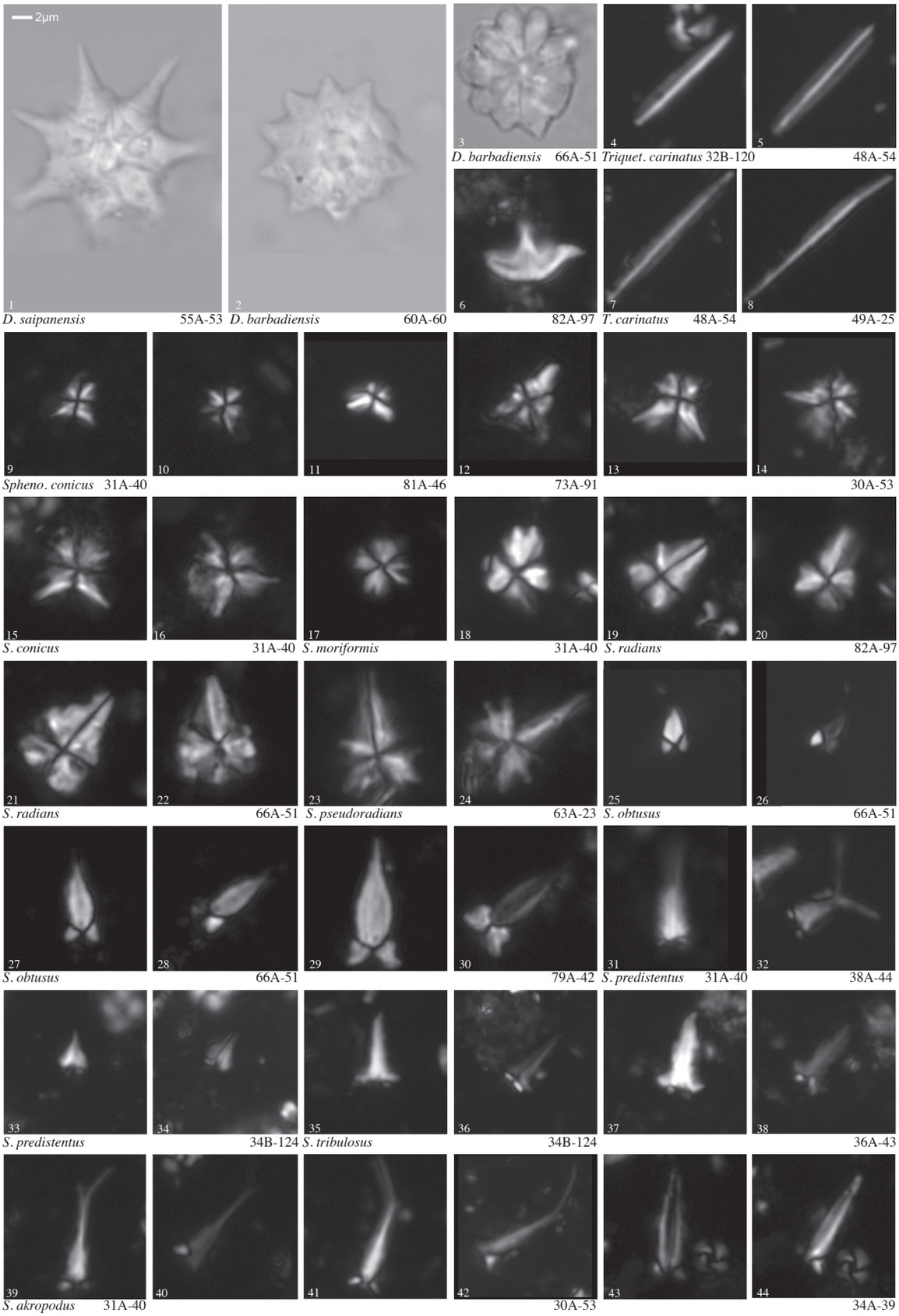

D. saipanensis 55A-53 *D. barbadiensis* 60A-60 *D. barbadiensis* 66A-51 *Triquet. carinatus* 32B-120 48A-54

82A-97 *T. carinatus* 48A-54 49A-25

Spheno. conicus 31A-40 81A-46 73A-91 30A-53

S. conicus 31A-40 *S. moriformis* 31A-40 *S. radians* 82A-97

S. radians 66A-51 *S. pseudoradians* 63A-23 *S. obtusus* 66A-51

S. obtusus 66A-51 79A-42 *S. predistentus* 31A-40 38A-44

S. predistentus 34B-124 *S. tribulosus* 34B-124 36A-43

S. akropodus 31A-40 30A-53 34A-39

Scyphosphaera expansa Bukry & Percival, 1971
Pl. 4, figs 16, 17

Family ZYGODISCACEAE Hay & Mohler, 1967

Neochiastozygus tenansa (Deflandre *in* Deflandre & Fert, 1954) Self-Trail, 2011
Pl. 5, figs 8–12

Family RHABDOSPHAERACEAE Haeckel, 1894

Blackites amplus Roth & Hay *in* Hay et al., 1967
Pl. 4, fig. 18

Blackites cf. *B. globosus* Bown, 2005
Pl. 4, figs 19, 20

Remarks: Small, squat and bulbous *Blackites*, with no observed basal coccolith. These were likely broken specimens, with missing or very short, hollow spines. No ornamentation was seen across the sphere.

Blackites culter? Dunkley Jones et al., 2009
Pl. 4, fig. 21

Remarks: Only one specimen was recorded, and the species was questionable due to the specimen having a slimmer spine and a missing basal coccolith.

Blackites gladius? (Locker, 1967) Varol, 1989
Pl. 4, fig. 25

Remarks: A single, broken specimen was recorded, hence the species identification is questionable.

Blackites inversus (Bukry & Bramlette, 1969) Bown & Newsam, 2017
Pl. 4, figs 33, 34

Blackites spiculiformis Bown & Dunkley Jones, 2006
Pl. 4, figs 22, 23

Blackites spinosus (Deflandre & Fert, 1954) Hay & Towe, 1962
Pl. 4, figs 29–32

Blackites stilus Bown, 2005
Pl. 4, figs 26, 27

Blackites subtilis? Bown & Newsam, 2017
Pl. 4, figs 35, 36

Remarks: The identification of this specimen was questionable because it appears to taper at both ends; according to the description in Bown & Newsam (2017), this species does *not* taper at the ends. However, the tapering may be due to the oblique angle causing a distorted view.

Blackites tenuis (Bramlette & Sullivan, 1961) Sherwood, 1974
Pl. 4, fig. 28

Blackites tortilis Bown & Dunkley Jones, 2006
Pl. 4, fig. 24

Order SYRACOSPHAERALES Hay, 1977 emend. Young et al., 2003
Family CALCIOSOLENIACEAE Kamptner, 1927

Calciosolenia alternans Bown & Dunkley Jones, 2006
Pl. 4, figs 37, 38

Family SYRACOSPHAERACEAE Lemmermann, 1908

Syracosphaera tanzanensis Bown, 2005
Pl. 4, figs 39, 40

6.3 Holococcoliths

Family CALYPTROSPHAERACEAE Boudreaux & Hay, 1967

Holodiscolithus minolettii Bown, 2005
Pl. 5, figs 5–7

Orthozygus aureus (Stradner, 1962) Bramlette & Wilcoxon, 1967
Pl. 5, figs 13–16

Lanternithus minutus Stradner, 1962
Pl. 5, figs 1–4

Zygrhablithus bijugatus subsp. *bijugatus* (Deflandre *in* Deflandre & Fert, 1954) Deflandre, 1959
Pl. 5, figs 19–24

Clathrolithus ellipticus Deflandre *in* Deflandre & Fert, 1954
Pl. 5, figs 17, 18

6.4 Extant nannoliths

Order BRAARUDOSPHAERALES Aubry, 2013
Family BRAARUDOSPHAERACEAE Deflandre, 1947

Braarudosphaera bigelowii (Gran & Braarud, 1935) Deflandre, 1947
Pl. 5, figs 25, 26

6.5 Extinct Nannoliths

Micrantholithus astrum? Bown, 2005
Pl. 5, fig. 27

Pemma basquense (Martini, 1959) Báldi-Beke, 1971
Pl. 5, figs 28, 29

Pemma papillatum Martini, 1959
Pl. 5, figs 30–32

Pemma triquetra Bown & Dunkley Jones, 2006
Pl. 5, figs 33, 34

Unknown nannolith
Pl. 5, figs 35, 36

Description: A form resembling a pinwheel, with five visible rays, although we suspected there were six rays in total, inferring that this nannolith possesses three pairs of triangular, overlapping segments. One segment in each pair goes extinct when rotated to 45°, revealing the segment division. At 0°, all the segments are bright. A small, circular central node is present, but has no outstanding features. **Occurrence**: CNO3 (NP23).

Order DISCOASTERALES Hay, 1977 emend. Bown, 2010
Family DISCOASTERACEAE Tan Sin Hok, 1927

Remarks: The overall preservation of this genus was not very good, making species identification problematic.

Discoaster barbadiensis Tan Sin Hok, 1927
Pl. 6, figs 2, 3, 6

Discoaster distinctus Martini, 1958
Pl. 5, figs 37, 38, 41

Discoaster nodifer (Bramlette & Riedel, 1954) Bukry, 1973
Pl. 5, figs 39, 40

Discoaster saipanensis Bramlette & Riedel, 1954
Pl. 6, fig. 1

Discoaster septemradiatus? (Klumpp, 1953) Martini, 1958
Pl. 5, fig. 42

Remarks: The rays appear to curve proximally. There was a possible underlying disc.

Discoaster tanii Bramlette & Riedel, 1954
Pl. 5, fig. 45

Discoaster tanii subsp. *ornatus* Bramlette & Wilcoxon, 1967
Pl. 5, figs 43, 44

Family SPHENOLITHACEAE Deflandre, 1952

Sphenolithus moriformis group
Pl. 6, figs 9–18

Sphenolithus conicus Bukry, 1971
Pl. 6, figs 9–16

Remarks: Small forms of this species were first documented in Upper Eocene sample NKK/1-54A (72.44 mbgl) in CNE19 (NP19/20), with larger forms appearing above, in the Lower Oligocene.

Sphenolithus moriformis (Brönnimann & Stradner, 1960) Bramlette & Wilcoxon, 1967
Pl. 6, figs 17, 18

Sphenolithus predistentus group
Pl. 6, figs 25–44

Sphenolithus akropodus de Kaenel & Villa, 1996
Pl. 6, figs 39–44

Remarks: The base of common *S. akropodus* was very close to the base of the Oligocene in CNO1 (NP21).

Sphenolithus obtusus Bukry, 1971
Pl. 6, figs 25–30

Sphenolithus predistentus Bramlette & Wilcoxon, 1967
Pl. 6, figs 31–34

Remarks: A great variation in the shape of the spine and in the size were observed. The specimens ranged from small to large, with spines that diverged distally.

Sphenolithus tribulosus Roth, 1970
Pl. 6, figs 35–38

Sphenolithus radians group
Pl. 6, figs 19–24

Sphenolithus radians Deflandre *in* Grassé, 1952
Pl. 6, figs 19–22

Sphenolithus pseudoradians Bramlette & Wilcoxon, 1967
Pl. 6, figs 23, 24

Nannoliths incertae sedis

Triquetrorhabdulus carinatus Martini, 1965
Pl. 6, figs 4, 5, 7, 8

Remarks: Occurred sporadically in both the Upper Eocene and Lower Oligocene sediments.

Acknowledgements

This project was funded by the CENTA Doctoral Training Programme as part of the Natural Environmental Research Council, Grant Code: NE/L002493/1. Special thanks to Dr Jeremy Young for taxonomic guidance and engaging discussions. We offer thanks to Professor Paul Pearson and the Java Drilling Team for our involvement in this project and providing sample material. We also thank Jean-Self Trail and an anonymous reviewer for their constructive comments and remarks. Nannofossil occurrence data is available online (at figshare: https://doi.org/10.6084/m9.figshare.12488783.v1).

References

Agnini, C., Fornaciari, E., Raffi, I., Catanzariti, R., Pälike, H., Backman, J. & Rio, D. 2014. Biozonation and biochronology of Paleogene calcareous nannofossils from low and middle latitudes. *Newsletters on Stratigraphy*, **47**: 131–181.

Aubry, M.-P. 1992a. Paleogene calcareous nannofossils from the Kerguelen Plateau, Leg 120. *Proceedings of the Ocean Drilling Programme, Scientific Results*, **120**: 471–491.

Aubry, M.-P. 1992b. Late Paleogene nannoplankton evolution: a tale of climatic deterioration. *In*: D.R. Prothero & W.A. Berggren (Eds). *Eocene–Oligocene Climatic and Biotic Evolution*. Princeton University Press, Princeton: 272–309.

Bergen, J., de Kaenel, E., Blair, S., Boesiger, T. & Browning, E. 2017. Oligocene-Pliocene taxonomy and stratigraphy of the genus *Sphenolithus* in the circum-North Atlantic Basin: Gulf of Mexico and ODP Leg 154. *Journal of Nannoplankton Research*, **37**(2–3): 77–112.

Berggren, W.A., Kent, D.V., Swisher, C.C., III & Aubry, M.-P. 1995. A revised Cenozoic geochronology and chronostratigraphy. *In*: W.A. Berggren, D.V. Kent, M.-P. Aubry & J. Hardenbol (Eds). Geochronology, Time Scales and Global Stratigraphic Correlation: Unified Temporal Framework for an Historical Geology. *Society for Sedimentary Geology*, **54**: 129–212.

Blaj, T., Backman, J. & Raffi, I. 2009. Late Eocene to Oligocene preservation history and biochronology of calcareous nannofossils from paleo-equatorial Pacific Ocean sediments. *Rivista Italiana de Paleontologia e Stratigrafia*, **115**(1): 67–85.

Bown, P.R. 2005. Cenozoic calcareous nannofossil biostratigraphy, ODP Leg 198 Site 1208 (Shatsky Rise, northwest Pacific Ocean). *Proceedings of Ocean Drilling Project, Scientific Results*, **198**: 1–44.

Bown, P.R. & Dunkley Jones, T. 2012. Calcareous nannofossils from the Paleogene equatorial Pacific (IODP Expedition 320 Sites U1331–1334). *Journal of Nannoplankton Research*, **32**(2): 3–51.

Bown, P.R., Dunkley Jones, T., Lees, J.A., Randell, R.D., Mizzi, J.A., Pearson, P.N., Coxall, H.K., Young, J.R., Nicholas, C.J., Karega, A., Singano, J. & Wade, B.S. 2008. A Paleogene calcareous microfossil Konservat-Lagerstätte from the Kilwa Group of coastal Tanzania. *Geological Society of America,*

Bulletin, **120**(1–2): 3–12.

Bown, P.R., Dunkley Jones, T. & Young, J.R. 2007. *Umbilicosphaera jordanii* Bown, 2005 from the Paleogene of Tanzania: Confirmation of generic assignment and a Paleocene origination for the family Calcidiscaceae. *Journal of Nannoplankton Research*, **29**: 25–30.

Bown, P.R., Lees, J.A. & Young, J.R. 2004. Calcareous nannoplankton evolution and diversity through time. *In*: H.R. Thierstein & J.R. Young (Eds). *Coccolithophores—From Molecular Processes to Global Impacts*. Springer, Berlin: 481–508.

Bown, P.R. & Newsam, C. 2017. Calcareous nannofossils from the Eocene North Atlantic Ocean (IODP Expedition 342 Sites U1403–1411). *Journal of Nannoplankton Research*, **37**(1): 25–60.

Bown, P.R. & Young, J.R. 1998. Techniques. *In*: P.R. Bown (Ed.). *Calcareous Nannofossil Biostratigraphy*. British Micropalaeontological Society Publications Series/Kluwer Academic, London: 16–28.

Bralower, T.J. 2005. Data report: Paleocene–early Oligocene calcareous nannofossil biostratigraphy, ODP Leg 198 Sites 1209, 1210, and 1211 (Shatsky Rise, Pacific Ocean). *In*: T.J. Bralower, I. Premoli Silva & M.J. Malone (Eds). *Proceedings of the Ocean Drilling Program, Scientific Results*, **198**: 1–15.

Bukry, D. 1971. Cenozoic calcareous nannofossils from the Pacific Ocean. *San Diego Society of Natural History Transactions*, **16**: 303–327.

Bukry, D. 1973. Low-latitude coccolith biostratigraphic zonation. *Initial Reports of the Deep-Sea Drilling Project*, **15**: 685–703.

da Gama, R. & Varol, O. 2014. New late Oligocene to Miocene species. *Journal of Nannoplankton Research*, **33**(1): 1–12.

De Deckker, P. 2016. The Indo-Pacific Warm Pool: Critical to world oceanography and world climate. *Geoscience Letters*, **3**(20): 1–12.

Deflandre, G. & Fert, C. 1954. Observations sur les Coccolithophoridés actuels et fossiles en microscopie ordinaire et électronique. *Annales de Paléontologie*, **40**: 115–176.

de Kaenel, E. & Villa, G. 1996. Oligocene-Miocene calcareous nannofossil biostratigraphy and paleoecology from the Iberian Abyssal Plain. *Proceedings of the Ocean Drilling Programme, Scientific Results*, **149**: 79–145.

Dunkley Jones, T., Bown, P.R. & Pearson, P. 2009. Exceptionally well preserved upper Eocene to lower Oligocene calcareous nannofossils (Prymnesiophycidae) from the Pande Formation (Kilwa Group), Tanzania. *Journal of Systematic Palaeontology*, **7**(4): 359–411.

Dunkley Jones, T., Bown, P.R., Pearson, P.N., Wade, B.S., Coxall, H.K. & Lear, C.H. 2008. Major shifts in calcareous phytoplankton assemblages through the Eocene-Oligocene transition of Tanzania and their implications for low-latitude primary production. *Palaeoceanography*, **23**: 1–14.

Fioroni, C., Villa, G., Persico, D. & Jovane, L. 2015. Middle Eocene–Lower Oligocene calcareous nannofossil biostratigraphy and paleoceanographic implications from Site 711 (equatorial Indian Ocean). *Marine Micropaleontology*, **118**: 50–62.

Fornaciari, E., Agnini, C., Catanzariti, R., Rio, D., Bolla, E.M. & Valvasoni, E. 2010. Mid-latitude calcareous nannofossil biostratigraphy and biochronology across the middle to late Eocene transition. *Stratigraphy*, **7**(4): 229–264.

Gradstein, F., Ogg, J., Schmitz, M. & Ogg, G. 2012. *The Geologic Timescale*. Elsevier, London. https://doi.org/10.1016/C2011-1-08249-8

Grassé, P.P. 1952. *Traité de Zoologie*. Masson, Paris: 1071 pp.

Hall, R. 2009. Southeast Asia's changing palaeogeography. *Blumea*, **54**: 148–161.

Hall, R. 2012. Late Jurassic–Cenozoic reconstructions of the Indonesian region and the Indian Ocean. *Tectonophysics*, **570-571**: 1–41.

Hall, R. 2013. The palaeogeography of Sundaland and Wallacea since the Late Jurassic. *Journal of Limnology*, **72**(s2): 1–17.

Hay, W.W., Mohler, H.P., Roth, P.H., Schmidt, R.R. & Boudreaux, J.E. 1967. Calcareous nannoplankton zonation of the Cenozoic of the Gulf Coast and Caribbean-Antillean area and transoceanic correlation. *Gulf Coast Association of Geological Societies, Transactions*, **17**: 428–480.

Huber, M. & Caballero, R. 2011. Eocene El Niño: Evidence for robust tropical dynamics in the 'hothouse'. *Science*, **299**(5608): 877–881.

Jones, A.P., Dunkley Jones, T., Coxall, H., Pearson, P.N., Nala, D. & Hoggett, H. 2019. Low-latitude calcareous nannofossil response in the Indo-Pacific Warm Pool across the Eocene–Oligocene Transition of Java, Indonesia. *Paleoceanography and Paleoclimatology*, **34**: 1–15.

Jones, A. & Dunkley Jones, T. 2020. Middle Eocene to Early Oligocene calcareous nannofossils from the Nanggulan Formation, Java, Indonesia. Supplementary data, figshare. https://doi.org/10.6084/m9.figshare.12488783.v1

Lunt, D.J., Dunkley Jones, T., Heinemann, M., Huber, M., LeGrande, A., Winguth, A., Loptson, C., Marotzke, J., Roberts,

C.D., Tindall, J., Valdes, P. & Winguth, C. 2012. A model–data comparison for a multi-model ensemble of early Eocene atmosphere–ocean simulations: EoMIP. *Climates of the Past*, **8**: 1717–1736.

Martini, E. 1971. Standard Tertiary and Quaternary calcareous nannoplankton zonation. *In*: A. Farinacci (Ed.). *Proceedings of the II Planktonic Conference, Roma, 1970. Edizioni Tecnoscienza*, **2**: 739–785.

Narciso, A., Cachão, M. & de Abreu, L. 2006. *Coccolithus pelagicus* subsp. *pelagicus* versus *Coccolithus pelagicus* subsp. *braarudii* (Coccolithophore, Haptophyta): A proxy for surface subarctic Atlantic waters off Iberia during the last 200 kyr. *Marine Micropaleontology*, **59**: 15–34.

Newsam, C., Bown, P.R., Wade, B.S. & Jones, H.L. 2017. Muted calcareous nannoplankton response at the Middle/Late Eocene turnover event in the western North Atlantic Ocean. *Newsletters on Stratigraphy*, **50**(3): 297–309.

Perch-Nielsen, K. 1985. Cenozoic calcareous nannofossils. *In*: H.M. Bolli, J.B. Saunders & K. Perch-Nielsen (Eds). *Plankton Stratigraphy*. Cambridge University Press, Cambridge: 427–554.

Persico, D., Fioroni, C. & Villa, G. 2012. A refined calcareous nannofossil biostratigraphy for the middle Eocene–early Oligocene Southern Ocean ODP sites. *Palaeogeography, Palaeoclimatology, Palaeoecology*, **335–336**: 12–23.

Renema, W., Bellwood, D.R., Braga, J.C., Bromfield, K., Hall, R., Johnson, K.G., Lunt, P., Meyer, C.P., McMonagle, L.B., Morley, R.J., O'Dea, A., Todd, J.A., Wesselingh, F.P., Wilson, M.E.J. & Pandolfi, J.M. 2008. Hopping hotspots: Global shifts in marine biodiversity. *Science,* **321**(5889): 654–657.

Self-Trail, J.M., Parker, M., Haynes, J.T., Schultz, A.P. & Huddlestun, P.F. 2019. Geology and biostratigraphy of the Upper Floridan aquifer in the greater Savannah region, Georgia and South Carolina. *Stratigraphy*, **16**: 41–62. doi:10.29041/strat.16.1.41-62

Shamrock, J.L. & Watkins, D.K. 2012. Eocene calcareous nannofossil biostratigraphy and community structure from Exmouth Plateau, Eastern Indian Ocean (ODP Site 762). *Stratigraphy*, **9**(1): 1–54.

Stradner, H. & Edwards, A.R. 1968. Electron microscopic studies on upper Eocene coccoliths from the Oamaru Diatomite, New Zealand. *Jahrbuch der Geologischen Bundesanstalt*, **13**: 1–66.

Villa, G., Fioroni, C., Pea, L., Bohaty, S. & Persico, D. 2008. Middle Eocene–late Oligocene climate variability: Calcareous nannofossil response at Kerguelen Plateau, Site 748. *Marine Micropaleontology*, **69**(2): 173–192.

Wei, W.C. & Wise, S.W. 1990. Biogeographic gradients of middle Eocene–Oligocene calcareous nannoplankton in the South Atlantic Ocean. *Palaeogeography, Palaeoclimatology, Palaeoecology*, **79**(1–2): 29–61.

Wise, S.W. 1983. Mesozoic and Cenozoic nannofossils recovered by DSDP Leg 71 in the Falkland Plateau region, southwest Atlantic Ocean. *Initial Reports of the Deep-Sea Drilling Project*, **71**: 481–550.

Young, J.R. 1998. Neogene. *In*: P.R. Bown (Ed.). *Calcareous Nannofossil Biostratigraphy*. British Micropalaeontological Society Publications Series, Chapman & Hall, London: 225–265.

Young, J.R., Bergen, J.A., Bown, P.R., Burnett, J.A., Fiorentino, A., Jordan, R.W., Kleijne, A., van Niel, B.E., Romein, A.J.T. & Von Salis, K. 1997. Guidelines for coccolith and calcareous nannofossil terminology. *Palaeontology*, **40**: 875–912.

Young, J.R. & Bown, P.R. 1997. Cenozoic calcareous nannoplankton classification. *Journal of Nannoplankton Research*, **19**: 36–47.

Young, J.R., Geisen, M., Cros, L., Kleijne, A., Sprengel, C., Probert, I. & Ostergaard, K.K. 2003. A guide to extant coccolithophore taxonomy. *Journal of Nannoplankton Research, Special Issue* **1**: 1–125.